第 50 卷 第 12 期/2023 年 6 月/中国激光 研究论文

中国激光

光纤激光-TIG复合焊接小孔型气孔的形成规律分析

赵振家，祝宝琦，邹江林*，郭士慧，孔华

北京工业大学材料与制造学部激光工程研究院高功率及超快激光先进制造实验室，北京 100124

摘要 本文基于焊接过程中线性提高激光功率的方法研究了光纤激光-TIG复合焊接焊缝中小孔型气孔的影响因素。结果表明，在复合焊接过程中将激光功率由0 kW线性增加至3 kW，可以获得激光功率和电弧电流对小孔型气孔的影响规律。当激光功率小于0.8 kW或大于2.2 kW时，焊缝内部均无小孔型气孔产生；当激光功率处于0.8～2.2 kW或保护气流量大于15 L/min时，焊缝内气孔相对较多，气孔率分别可达3.5%和5.5%；当激光功率为2 kW时，150 A的TIG电弧电流使熔宽提高了94%，熔深提高了35%，并控制了飞溅数量，改善了焊缝表面成形质量。进一步分析表明：电弧作用于小孔口的力是增加小孔不稳定性、提高焊缝中小孔型气孔数量的主要原因；激光功率变化导致孔内激光致蒸发量的变化是复合焊接焊缝中气孔数量改变的主要因素。

关键词 激光技术；光纤激光；复合焊接；小孔型气孔；工艺参数

中图分类号 TG456.7 **文献标志码** A **DOI**：10.3788/CJL221115

1 引 言

激光-电弧复合焊接技术是一种综合了激光焊与电弧焊各自优点的焊接方法，具有高桥联性、高间隙适应性等优势[1-4]。此外，激光与电弧这两种热源可以产生“1+1>2”的协同增强效应，故而可以获得更大的焊接熔深或更高的焊接效率[5-8]。目前，激光-电弧复合焊接技术已在航空航天、轨道交通和国防武器等行业受到广泛关注。然而，大量研究发现，激光-电弧复合焊接过程中依然存在气孔、飞溅等焊接缺陷[9-12]。其中，气孔的存在会削弱焊缝的有效工作截面，对接头的强韧性产生严重的负面影响[13]。因此，研究激光-电弧复合焊接过程中气孔的影响因素，对于进一步理解复合焊接物理过程以及优化复合焊接工艺参数具有重要意义。

焊缝中的气孔主要分为冶金气孔和小孔型气孔[14-15]。其中：冶金气孔一般集中在焊缝中上部，形状为规则的圆形，尺寸较小；小孔型气孔的尺寸明显大于冶金气孔，且形状不规则，通常为激光致深熔小孔坍塌所致[16]。深熔小孔内激光致蒸气（羽辉）喷发是影响深熔小孔坍塌的关键因素之一。国内外研究人员对激光-电弧复合焊接进行了广泛研究：Li等[17]采用高速相机对羽辉的形状和波动情况进行观察，以此间接研究深熔小孔的稳定性；Casalino等[18]在光纤激光-MIG复合焊接铝合金过程中发现较高的激光功率有利于维持小孔稳定和减少焊缝中的小孔型气孔；Sun等[19]在脉冲激光-TIG复合焊接过程中发现，脉冲激光能量是影响焊接缺陷的关键因素，合适的电弧电流能有效减少气孔；Ola等[20]发现激光功率密度会影响小孔的形状和尺寸，进而影响气孔率；Katayama等[21]发现增大电弧电流能使熔池表面下凹，减小气泡逸出距离，延长熔池存在和凝固的时间，从而减小焊缝气孔率；雷正龙等[22]发现，在激光-MIG复合焊接时采用激光在前的引导方式，焊缝中的气孔数量较少；王红阳等[23]在激光-TIG高速复合焊接6061-T6过程中发现，熔池冷却状态的改变易导致小孔稳定性降低并发生坍塌；蔡创等[24]在激光-MIG复合焊接铝合金时引入摆动激光，不仅增强了小孔的稳定性，还使熔池底部的气泡快速逸出，降低了焊缝气孔率；韩晓辉等[25]发现增大热源与焊接方向的夹角有利于减少气孔；张正浩等[26]发现复合焊接时提高焊速和增大离焦量能够显著减小气孔尺寸并减少气孔数量；李伟等[27]发现合适的工艺参数能够使气泡有足够的时间和空间从焊缝中逃逸。

本课题组采用IPG YLS-6000光纤激光器与旁轴TIG电弧焊机对低碳钢进行平板扫描焊接试验，研究了焊缝中小孔型气孔的影响因素。首先采用线性变激光功率方法探究了激光致蒸气对复合焊接小孔型气孔的影响规律；随后结合高速摄像观测了复合焊接等离子体的形态，研究了电弧对小孔型气孔的影响；最后综合复合焊接熔深、熔宽、焊缝成形质量、焊缝气孔率的变化规律，分析了光纤激光-TIG复合焊接焊缝中小孔型气孔的形成规律和影响因素。

收稿日期：2022-08-08；**修回日期**：2022-08-31；**录用日期**：2022-09-05；**网络首发日期**：2022-09-20

基金项目：国家自然科学基金面上项目（51875007）、北京市自然科学基金面上项目（3222004）

通信作者：*zoujianglin1@163.com

2 试验方法及设备

试验采用的是 IPG YLS-6000 光纤激光器，其输出激光的波长为 1.07 μm。光纤传输芯径为 200 μm，输出耦合准直镜的焦距为 200 mm。激光经焦距为 300 mm 的聚焦系统聚焦后获得焦斑直径约为 0.3 mm 的光束。焊接过程中光纤激光束的离焦量为 0 mm。运动系统采用的是 DMC-B140-M 控制系统控制的移动平台（美国 GALIL 公司）。采用 YC-315TX 型直流 TIG 焊机，直流正接。选用直径为 2.4 mm 的钍钨极，其尖端距离工件表面 2 mm。焊枪与激光束之间的夹角为 45°，激光束中心轴与钨极尖端的间距 D_{LA} 为 2 mm。试验中采用激光在前电弧在后的复合焊接方式。FASTCAM Mini UX100 高速摄像机放置在垂直于激光电弧平面的位置处进行电弧形态记录，拍摄帧率为 5000 frame/s。试验装置布置如图 1 所示。

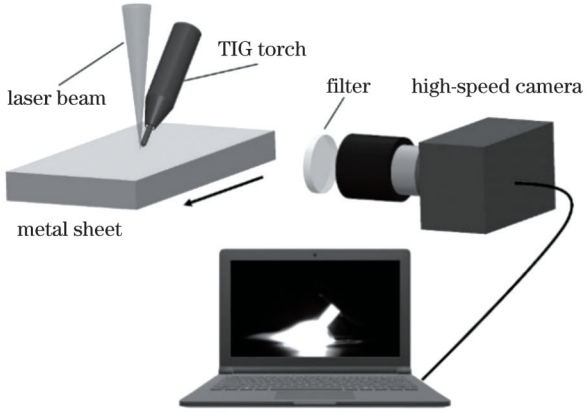

图 1 复合焊接示意图

Fig. 1 Schematic diagram of hybrid welding

试验中焊接速度固定为 2 m/min，保护气采用氩气。如图 1 所示，高速摄像机前配置透光率为 25% 的中性衰减片，以观测复合焊接等离子体。试验用待焊接材料是尺寸为 100 mm×50 mm×10 mm 的 Q235 低碳钢板，板材表面无涂层；Q235 低碳钢板的化学成分如下：0.12%C，0.33%Mn，≤0.30%Si，≤4.50%S，≤4.50%P，其余为铁。焊接前，采用磨削的方式对母材进行表面处理，然后进行丙酮擦拭，以去除钢板表面的杂质。各焊接参数下重复进行 3 次焊接试验。对焊接样品的焊缝进行纵向切割、磨抛和腐蚀，然后采用 KEYENCE VHX-950 光学显微镜（OM）进行焊缝表面形貌拍摄，并使用配套软件测量焊缝的熔深、熔宽。使用 Image J 软件对照片上的气孔面积与焊缝面积信息进行采集与计算。本文将焊缝气孔投影总面积与焊缝投影面积的比值作为气孔率，计算公式为

$$P=\frac{\sum_{p=1}^{n}S_p}{S_w}, \tag{1}$$

式中：P 为焊缝气孔率；S_p 为单个气孔的投影面积；S_w 为焊缝投影面积。

3 试验结果

3.1 激光致蒸发量与复合焊接气孔的关系

在焊接过程中，激光功率在 2 s 内由 0 kW 线性增大至 3 kW，保护气流量为 10 L/min，电弧电流（I）分别设置为 0、100、150 A。焊后沿焊缝中心线纵向剖开，观察焊缝纵向形貌，结果如图 2 所示。可见：在不同的电弧电流下，焊接熔深均随着激光功率的增加而增大；单激光焊接（电弧电流为 0 A）时，焊缝中几乎没有气孔；当电弧电流为 100 A 和 150 A 时，焊缝中部和下部区域存在大量气孔，气孔密集，气孔形状不规则且尺寸较大，可确定为小孔型气孔。另外，由图 2 还可以看出：当激光功率小于 0.8 kW 时，焊缝内部几乎无气孔；当激光功率大于 2.2 kW 时，焊缝中的气孔几乎全部消失。

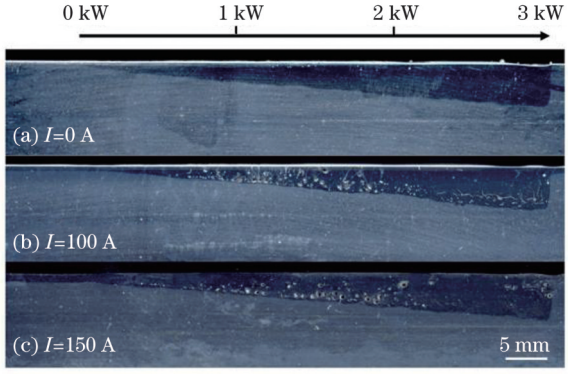

图 2 焊缝纵向截面的熔深对比

Fig. 2 Comparison of weld vertical section penetration

固定电弧电流为 150 A，改变激光功率进行复合焊接试验，获得了不同激光功率下复合焊接焊缝中心的纵截面形貌，如图 3 所示。分析图 3 可以发现：当激光功率不大于 0.8 kW 时，焊缝内部几乎无气孔；当激光功率为 4 kW 时，焊缝内部无气孔；当激光功率在 1～2.2 kW 范围时，焊缝中部分布着较为密集的不规则状气孔。该结果与图 2 所示结果几乎是一致的，即：当激光功率较低或较高时，焊缝内部几乎没有气孔；当激光功率取中间值时，焊缝内部的小孔型气孔分布较为密集。所以在试验过程中采用线性变激光功率复合焊接的方式来研究气孔分布区间的变化是可行的，并且采用这种方式能够减少试验量。

基于图 3 测量不同激光功率下的焊缝气孔率，得到了气孔率随激光功率的变化规律，如图 4 所示。可以发现：当激光功率为 0.5 kW 时气孔率仅为 0.05%，当激光功率为 0.8 kW 时气孔率增至 0.46%；之后气孔率随着激光功率继续增大而迅速增大，当激光功率为 1.4 kW 时，气孔率达到最大，为 3.5%；之后气孔率随着激光功率的增大而逐渐减小，当激光功率为 2.5 kW 时气孔率减小至 0.5%，当激光功率为 4 kW 时焊缝内部无

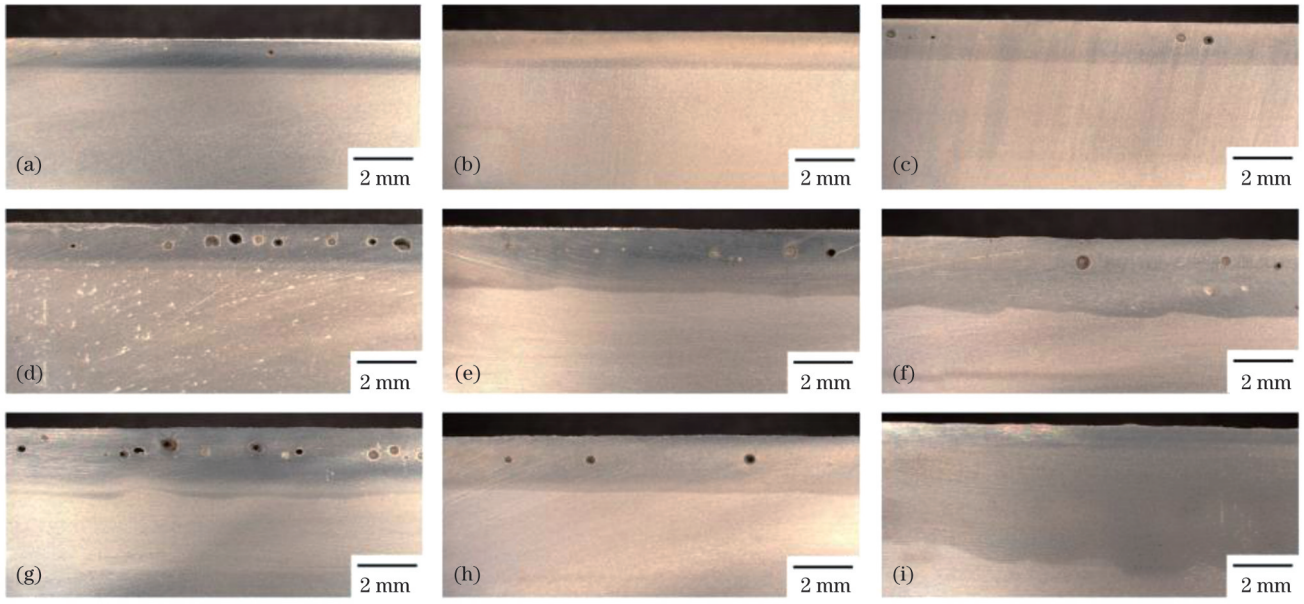

图 3　不同激光功率下激光-TIG 复合焊接焊缝中心的纵截面形貌。(a) 0.8 kW;(b) 1 kW;(c) 1.2 kW;(d) 1.4 kW;(e) 1.6 kW;(f) 1.8 kW;(g) 2 kW;(h) 2.2 kW;(i) 4 kW

Fig. 3　Vertical section images of weld center by laser TIG hybrid welding at different laser powers. (a) 0.8 kW; (b) 1 kW; (c) 1.2 kW; (d) 1.4 kW; (e) 1.6 kW; (f) 1.8 kW; (g) 2 kW; (h) 2.2 kW; (i) 4 kW

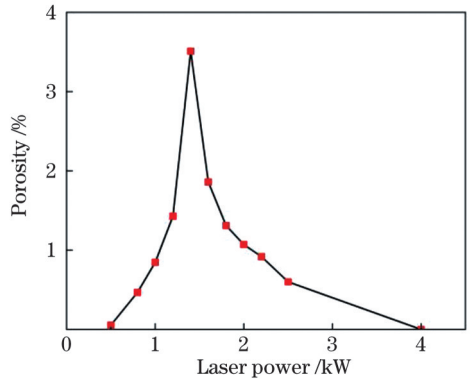

图 4　气孔率随激光功率的变化规律

Fig. 4　Variation of porosity with laser power

气孔产生。

3.2　电弧保护气流量对气孔率的影响

固定激光功率为 1.5 kW,电弧电流为 150 A,改变电弧保护气的流量进行试验,采用高速摄像机从侧面观察,获得不同保护气流量下典型的等离子体形态,如图 5 所示。可以看出,复合焊接等离子体的温度由内向外逐渐降低[28],等离子体发光强度、波长分别随着温度的升高而增大、变短。复合焊接等离子体温度高的区域集中于钨极尖端正下方,呈现亮白色,中上部橘黄色部分是温度较低的羽辉区域。随着保护气流量增大,上部橘黄色羽辉逐渐消失,下部亮白色等离子体逐渐减小。

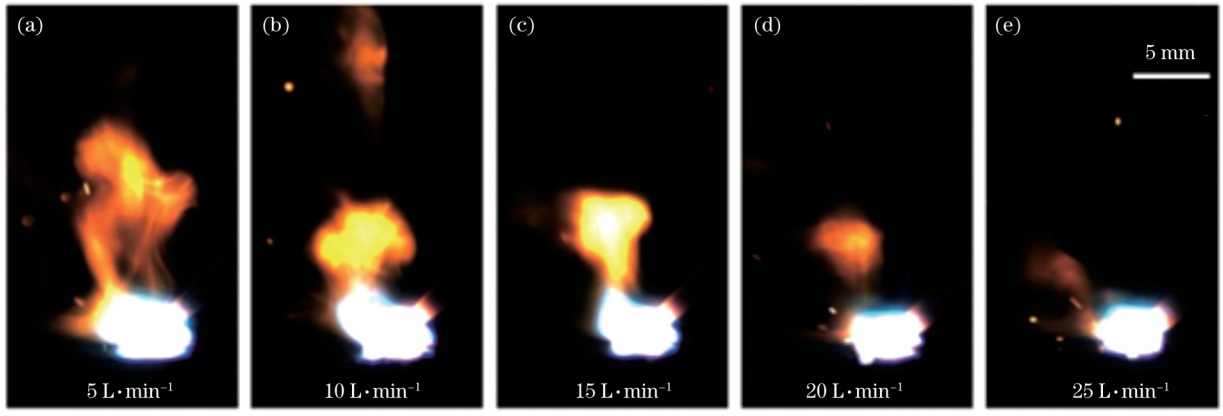

图 5　不同电弧保护气流量下的等离子体对比

Fig. 5　Comparison of plasma with different arc shielding gas flow

不同电弧保护气流量下焊缝纵向截面内部气孔分布与焊缝表面形貌如图 6 所示。随着电弧保护气流量增加,焊缝中心出现了一些不连续的凹坑,焊缝表面成形变差,焊缝内部气孔数量显著增多。当电弧保护气流量较小时,焊缝内部气孔多集中于焊缝中上部;当电弧保护气流量为 25 L/min 时,焊缝内部出现大量气

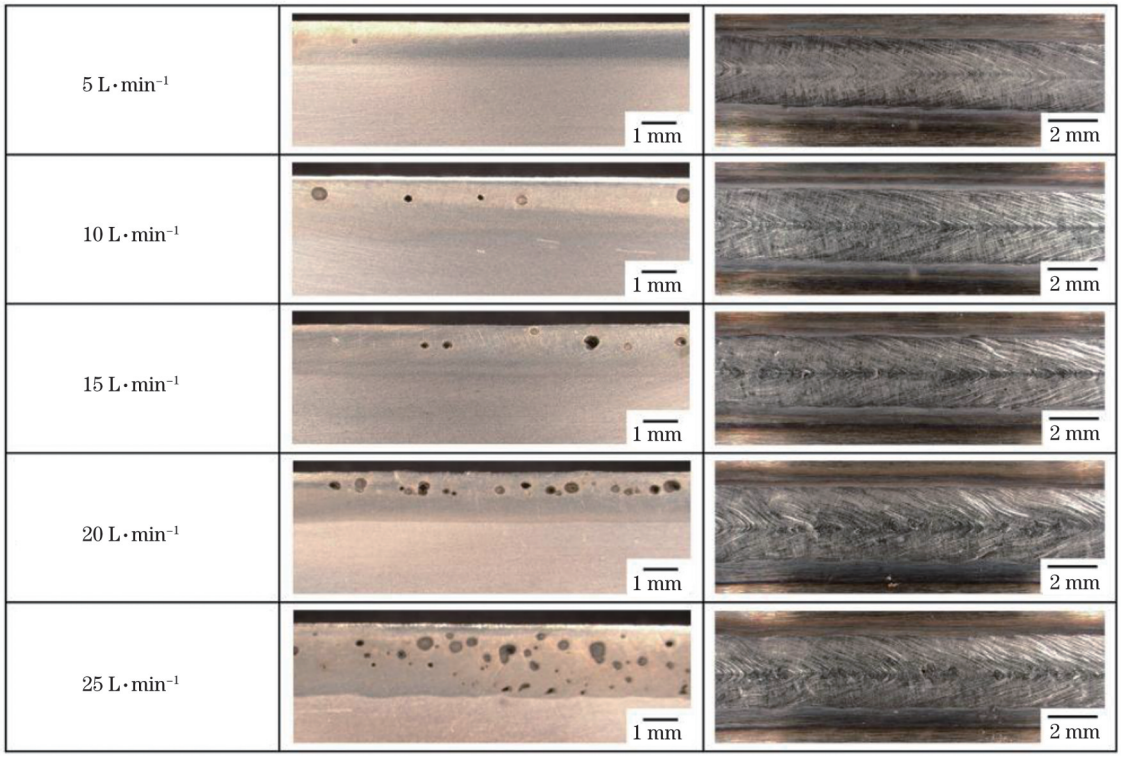

图 6　不同电弧保护气流量下焊缝内部气孔分布与焊缝表面形貌

Fig. 6　Pore distribution and weld surface morphology in weld under different arc shielding gas flows

孔，此时气孔多数集中于焊缝中部，焊缝底部也出现了不规则形状的气孔。

气孔率随电弧保护气流量的变化如图 7 所示。随着保护气流量从 5 L/min 增加到 25 L/min，气孔率从 0.25% 逐渐增大到 5.5%，并且气孔率与保护气流量近似呈一次线性关系。测量焊缝表面宽度后发现，随着保护气流量从 5 L/min 增加到 25 L/min，焊缝表面宽度从 3.01 mm 增加到 3.24 mm。这一现象表明通过提高保护气的流量来增大电弧作用于熔池/小孔口的力，能够明显增大焊缝的气孔率，并且过大的保护气流量能够影响焊缝表面宽度。

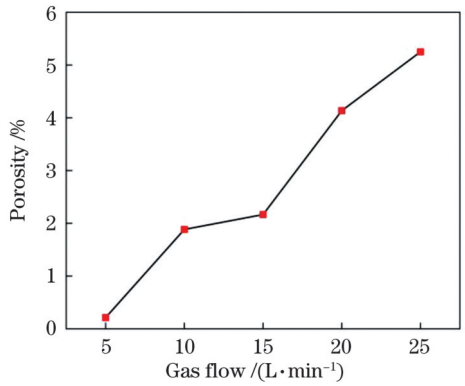

图 7　气孔率随电弧保护气流量的变化规律

Fig. 7　Variation of porosity with arc shielding gas flow

3.3　激光功率对复合焊接熔宽/熔深的影响因素

将激光功率设置为在 2 s 内由 0 kW 线性增至 3 kW，保护气流量为 10 L/min，电弧电流分别为 0、100、150 A，进行焊接试验，获得的典型焊缝形貌如图 8 所示。图中 I=0 A 表示单激光焊接。单激光焊接时，飞溅多，焊缝咬边较严重，焊缝成形质量较差。引入电弧后，复合焊接焊缝明显变宽，焊缝成形美观，呈致密的鱼鳞状条纹，几乎无飞溅、咬边等情况出现。这表明电弧的引入对高功率光纤激光焊接焊缝表面成形具有明显的改善作用。

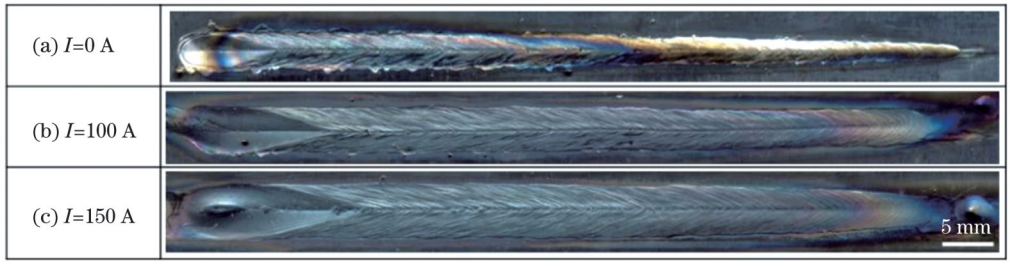

图 8　焊缝成形对比

Fig. 8　Comparison of weld formation

测量上述焊接参数下的焊缝熔宽，可得到熔宽随激光功率的变化规律，如图 9 所示。可见，熔宽随着激光功率和电弧电流的增加而增大。熔宽随电流增加而增大的原因是：TIG 电弧的加入增大了作用面积，且作用区随电流的增加而增大。熔宽随激光功率增加而增大与输入的能量增大有关。

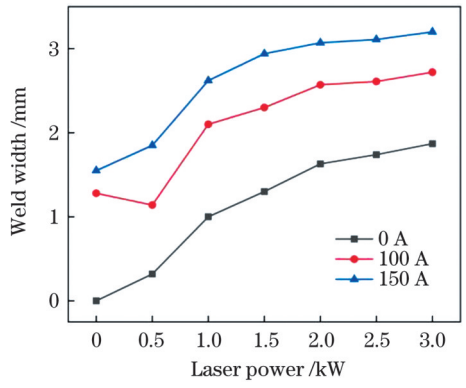

图 9 TIG 电流对焊缝熔宽的影响

Fig. 9 Influence of TIG current on weld width

不同电弧电流下焊接熔深随激光功率的变化规律如图 10 所示。可见，熔深与激光功率的关系基本呈线性正相关关系。当激光功率低于 0.8 kW 时，电流越大，对应的熔深越大；当激光功率达到 2 kW 时，150 A 的 TIG 电弧使熔宽提高了 94%，熔深提高了约 35%（与单激光焊接相比）；当激光功率增加到约 2.4 kW 时，复合焊接熔深明显大于单激光焊接熔深，但不同电流（100 A 和 150 A）对熔深影响的差距几乎消失。

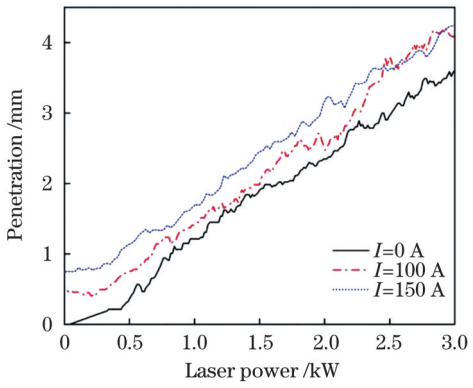

图 10 不同 TIG 电流下熔深随激光功率的变化规律

Fig. 10 Variation of penetration with laser power at different TIG currents

4 分析和讨论

激光焊接小孔型气孔的形成与深熔小孔的失稳、坍塌以及熔池凝固时孔内气体来不及逸出有关[29]。在光纤激光-TIG 复合焊接过程中，影响小孔稳定的力包括孔内激光致蒸气喷发时作用于孔壁的力与电弧作用于小孔口的力，如图 11 所示。由图 2 可知，单光纤激光焊接（没有电弧作用于熔池的力）时，焊缝中几乎没有气孔存在。这表明仅有孔内激光致蒸气对孔壁熔池施加力时，更有利于提高小孔的稳定性或维持小孔不坍塌（相比于本文条件下的复合焊接），故而孔内激光致蒸气（即激光功率越大）越多，焊缝中的气孔越少。由图 6、图 7 可知，电弧作用于熔池的力越大（保护气流量越大），深熔小孔越易失稳、坍塌，故而焊缝中的气孔越多。

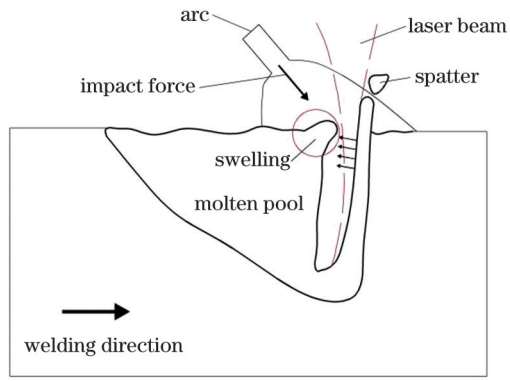

图 11 金属蒸气与小孔后壁的关系

Fig. 11 Relationship between metal vapor and back wall of keyhole

上述分析表明孔内激光致蒸气喷发时作用于孔壁熔池的力在维持小孔稳定性（不坍塌）方面表现为正面作用，而电弧作用于熔池的力在维持小孔稳定性（不坍塌）方面表现为负面作用。由图 5 可知当保护气流量为 5 L/min 时橘黄色羽辉喷发得较高，这是孔内激光致喷发蒸气（羽辉）流强于电弧保护气流所致；当保护气流量为 25 L/min 时橘黄色羽辉几乎消失，这是电弧保护气的流动吹除孔内喷发蒸气（羽辉）所致。因此，可以推测在适宜的参数下复合焊接过程中这两种气流可建立一种平衡状态，激光功率或电弧气流的变化均可打破该平衡。

在光纤激光-TIG 复合焊接中，当激光功率较低时，焊接模式为激光辅助电弧焊接、电弧主导焊接过程。尽管此时电弧作用于熔池的气流可能较孔内喷发蒸气流对小孔稳定性的影响更大，但此时小孔深度较浅，孔内蒸气较少且易逸出，故而小孔不易坍塌，焊缝中几乎没有小孔型气孔，如图 2 所示。当激光功率增加至典型的电弧辅助激光的复合焊接模式（激光为主）时，复合焊接过程表现出单激光焊接的特征，深熔小孔较深，孔内激光致蒸发量较大，此时孔内激光致蒸气喷发气流对小孔稳定性的影响较电弧保护气流更强，深熔小孔稳定性较高，孔内蒸气易于逸出，故而焊缝内部小孔型气孔少，如图 2 所示。

在光纤激光深熔焊接过程中，激光束直接作用于小孔前壁，前壁表面激光致蒸气将冲击小孔后壁，在小孔口后壁形成凸起液柱[30]。考虑到深熔小孔对入射激光的吸收率可达 90%[31]，金属熔池对电弧的吸收率约为 50%[32]，当激光功率在 0.8～2 kW 之间时，可认为激

光功率与电弧功率(电弧功率约为2.1 kW)大致相当,即该阶段处于复合焊接模式从激光为辅(电弧为主)转变为激光为主(电弧为辅)的过渡阶段。此时电弧作用于小孔口后壁凸起液柱的力(与孔内激光致蒸气的喷发相比)不可忽略。当电弧作用于小孔后沿凸起液柱的力过大时,该力将小孔口后部凸起液柱压向小孔口,如图11所示。此时,小孔口缩小,不利于孔内蒸气逸出。这是激光功率与电弧功率大致相当时,焊缝中出现大量小孔型气孔的原因。随着保护气流量进一步增大,电弧作用于小孔后沿的力更大,小孔口缩小,不利于孔内蒸气逸出,小孔发生失稳。这是随着保护气流量增加焊缝中小孔型气孔增多的原因。

光纤激光-TIG复合焊焊缝的熔宽、熔深较单光纤激光焊接均有明显增大,焊缝表面成形质量和飞溅也均有明显改善,如图8~10所示。TIG电弧的加入增加了作用面积,且作用区随电流的增加而增大,这是熔宽随电流增加而增大的原因。当激光功率较低时,这种复合焊接表现为以激光为辅、电弧为主的模式[33],故而电流越大,熔深越深。当激光功率增加到约2.4 kW时,本文试验条件下这种复合焊接模式是典型的以激光为主要热源、电弧为辅助热源的复合焊接模式。在该复合焊接模式下,电弧的主要作用是消除孔外羽辉对焊接过程的负面影响,故而复合焊接熔深较单激光焊接熔深更大。电弧的作用是去除羽辉的负面影响,故而熔深的大小与引入的电流的相关性不明显[16],主要由激光功率决定。

5 结 论

在复合焊接过程中使激光功率在2 s内由0 kW线性增加至3 kW可获得焊缝中小孔型气孔随激光功率的变化规律。激光功率小于0.8 kW或大于2.2 kW时,焊缝内部均无明显的小孔型气孔产生;当激光功率为0.8~2.2 kW或保护气流量大于15 L/min时,焊缝内小孔型气孔较多,气孔率分别可达3.5%和5.5%。

TIG电弧的引入明显改善了光纤激光焊接的焊缝成形质量,大幅提高了熔深和熔宽;当激光功率为2 kW时,150 A的TIG电弧电流使焊缝熔宽提高了94%,熔深提高了约35%(与单激光焊接相比)。

光纤激光-TIG电弧复合焊接焊缝中产生的小孔型气孔是电弧作用于小孔口导致小孔失稳、坍塌所致。增加保护气流量能够明显增加焊缝的气孔率。激光功率变化导致孔内激光致蒸发量变化是复合焊接焊缝中气孔数量改变的主要因素。

参 考 文 献

[1] Gao M, Zeng X Y, Hu Q W, et al. Laser-TIG hybrid welding of ultra-fine grained steel[J]. Journal of Materials Processing Technology, 2009, 209(2): 785-791.

[2] Ribic B, Palmer T A, DebRoy T. Problems and issues in laser-arc hybrid welding[J]. International Materials Reviews, 2009, 54(4): 223-244.

[3] Yan J, Gao M, Zeng X Y. Study on microstructure and mechanical properties of 304 stainless steel joints by TIG, laser and laser-TIG hybrid welding[J]. Optics and Lasers in Engineering, 2010, 48(4): 512-517.

[4] Rethmeier M, Gook S, Lammers M, et al. Laser-hybrid welding of thick plates up to 32 mm using a 20 kW fibre laser[J]. Quarterly Journal of the Japan Welding Society, 2009, 27(2): 74-79.

[5] Wu S K, Xiao R S. Effect of high power CO_2 and Yb∶YAG laser radiation on the characteristics of TIG arc in atmospherical pressure argon and helium[J]. Optics & Laser Technology, 2015, 67: 169-175.

[6] Naito Y, Mizutani M, Katayama S. Penetration characteristics in YAG laser and TIG arc hybrid welding, and arc and plasma/plume behaviour during welding: welding phenomena in hybrid welding using YAG laser and TIG arc (first report) [J]. Welding International, 2006, 20(10): 777-784.

[7] 陈彦宾, 陈杰, 李俐群, 等. 激光与电弧相互作用时的电弧形态及焊缝特征[J]. 焊接学报, 2003, 24(1): 55-56, 60.
Chen Y B, Chen J, Li L Q, et al. Properties of arc and weld in laser-TIG hybrid process[J]. Transactions of the China Welding Institution, 2003, 24(1): 55-56, 60.

[8] Zou J L, Wu S K, Xiao R S, et al. Effects of a paraxial TIG arc on high-power fiber laser welding[J]. Materials & Design, 2015, 86: 321-327.

[9] 吴世凯, 肖荣诗, 杨武雄, 等. 高功率CO_2及Yb∶YAG激光与TIG电弧相互作用特性对比[J]. 中国激光, 2010, 37(10): 2667-2671.
Wu S K, Xiao R S, Yang W X, et al. Characteristics comparison of laser-TIG arc interaction using high power CO_2 and Yb∶YAG laser[J]. Chinese Journal of Lasers, 2010, 37(10): 2667-2671.

[10] Song G, Luo Z M. The influence of laser pulse waveform on laser-TIG hybrid welding of AZ31B magnesium alloy[J]. Optics and Lasers in Engineering, 2011, 49(1): 82-88.

[11] Mahrle A, Beyer E. Hybrid laser beam welding: classification, characteristics, and applications[J]. Journal of Laser Applications, 2006, 18(3): 169-180.

[12] Liu L M, Chen M H, Li C B. Effect of electric arc on laser keyhole behavior based on direct observation during low power pulsed laser-arc hybrid welding process[J]. Optics and Lasers in Engineering, 2013, 51(10): 1153-1160.

[13] Zhao H Y, He L G, Niu W C, et al. Investigation on porosity suppression in deep-penetration laser welding by using computational fluid dynamics[J]. Journal of Laser Applications, 2016, 28(3): 032011.

[14] Zhou S J, Ling W L, Ma W P, et al. The pores formation mechanism in the laser-MIG hybrid welded joint of mild steel[J]. Materials Research Express, 2019, 6(9): 095803.

[15] 张迪, 赵琳, 刘奥博, 等. 激光能量对激光焊接接头熔化形状、气孔和微观组织的影响及其调控方法[J]. 中国激光, 2021, 48(15): 1502005.
Zhang D, Zhao L, Liu A B, et al. Understanding and controlling the influence of laser energy on penetration, porosity, and microstructure during laser welding[J]. Chinese Journal of Lasers, 2021, 48(15): 1502005.

[16] Atabaki M M, Ma J, Liu W, et al. Pore formation and its mitigation during hybrid laser/arc welding of advanced high strength steel[J]. Materials & Design, 2015, 67: 509-521.

[17] Li K, Lu F G, Guo S T, et al. Porosity sensitivity of A356 Al alloy during fiber laser welding[J]. Transactions of Nonferrous Metals Society of China, 2015, 25(8): 2516-2523.

[18] Casalino G, Mortello M, Leo P, et al. Study on arc and laser powers in the hybrid welding of AA5754 Al-alloy[J]. Materials & Design, 2014, 61: 191-198.

[19] Sun J, Wang H Y, Liu L M. The analysis on the formation of porosity during pulsed laser-induced TIG hybrid welding of 6061 aluminium alloy at high welding speed[J]. International Journal of Precision Engineering and Manufacturing, 2020, 21(8): 1469-1477.

[20] Ola O T, Doern F E. Factors controlling keyhole-induced porosity in cold wire laser welded aluminum[J]. Journal of Laser Applications, 2017, 29(1): 012008.
[21] Katayama S, Uchiumi S, Mizutani M, et al. Penetration and porosity prevention mechanism in YAG laser-MIG hybrid welding [J]. Welding International, 2007, 21(1): 25-31.
[22] 雷正龙, 黎炳蔚, 周恒, 等. 端接接头激光-MAG复合焊熔滴过渡与气孔特征分析[J]. 中国激光, 2019, 46(3): 0302007.
Lei Z L, Li B W, Zhou H, et al. Analysis of droplet transfer and porosity characteristics in laser-MAG hybrid welding of edge joint [J]. Chinese Journal of Lasers, 2019, 46(3): 0302007.
[23] 王红阳, 孙佳, 刘黎明. 6061-T6铝合金激光-电弧复合高速焊气孔形成及控制机制[J]. 中国激光, 2018, 45(3): 0302001.
Wang H Y, Sun J, Liu L M. Formation and controlling mechanism of pores in laser-TIG hybrid welding of 6061-T6 aluminum alloys at high peed[J]. Chinese Journal of Lasers, 2018, 45(3): 0302001.
[24] 蔡创, 谢佳, 刘致杰, 等. 铝合金摆动激光-MIG复合焊接特性及气孔控制[J]. 中国激光, 2021, 48(18): 1802002.
Cai C, Xie J, Liu Z J, et al. Welding characteristics and porosity control of weaving laser-MIG hybrid welding of aluminum alloys [J]. Chinese Journal of Lasers, 2021, 48(18): 1802002.
[25] 韩晓辉, 张志毅, 马国龙, 等. 热源角度对6A01铝合金激光-MIG复合焊成形及气孔的影响[J]. 中国激光, 2022, 49(2): 0202020.
Han X H, Zhang Z Y, Ma G L, et al. Effects of heat source angle on weld formation and porosity defects of laser-MIG hybrid welding of 6A01 aluminum alloy[J]. Chinese Journal of Lasers, 2022, 49(2): 0202020.
[26] 张正浩, 王传强, 齐恩语, 等. 核级高硅含钛不锈钢激光-电弧复合焊接工艺及接头组织性能[J]. 中国激光, 2021, 48(14): 1402008.
Zhang Z H, Wang C Q, Qi E Y, et al. Laser-arc hybrid welding process and joint microstructure and properties of nuclear grade high silicon titanium-containing stainless steel[J]. Chinese Journal of Lasers, 2021, 48(14): 1402008.
[27] 李伟, 朱加雷, 李志波, 等. 激光电弧复合焊接气孔控制方法的探索[J]. 应用激光, 2018, 38(3): 425-429.
Li W, Zhu J L, Li Z B, et al. Exploration of porosity control method for laser arc composite welding[J]. Applied Laser, 2018, 38(3): 425-429.
[28] Zhao Y Q, Zhan X H, Zhou X D, et al. Effect of heat input on macro morphology and porosity of laser-MIG hybrid welded joint for 5A06 aluminum alloy[J]. The International Journal of Advanced Manufacturing Technology, 2021, 115(11): 4035-4045.
[29] Xiao R S, Zhang X Y. Problems and issues in laser beam welding of aluminum-lithium alloys[J]. Journal of Manufacturing Processes, 2014, 16(2): 166-175.
[30] Zou J L, Zhu B Q, Zhang G L, et al. Power density effect on the laser beam-induced eruption of spatters in fiber laser keyhole welding[J]. Optics & Laser Technology, 2022, 147: 107651.
[31] Kawahito Y, Matsumoto N, Abe Y, et al. Relationship of laser absorption to keyhole behavior in high power fiber laser welding of stainless steel and aluminum alloy[J]. Journal of Materials Processing Technology, 2011, 211(10): 1563-1568.
[32] Wu D S, Tashiro S, Hua X M, et al. Analysis of the energy propagation in the keyhole plasma arc welding using a novel fully coupled plasma arc-keyhole-weld pool model[J]. International Journal of Heat and Mass Transfer, 2019, 141: 604-614.
[33] Mahrle A, Rose S, Schnick M, et al. Laser-assisted plasma arc welding of stainless steel[J]. Journal of Laser Applications, 2013, 25(3): 032006.

Analysis of Formation Law of Keyhole Porosity During Fiber Laser-TIG Hybrid Welding

Zhao Zhenjia, Zhu Baoqi, Zou Jianglin*, Guo Shihui, Kong Hua

High-Power and Ultrafast Laser Manufacturing Lab, Institute of Laser Engineering, Faculty of Materials and Manufacturing, Beijing University of Technology, Beijing 100124, *China*

Abstract

Objective Laser-arc hybrid welding combines a low-cost process-stable arc heat source with a highly efficient laser heat source, reducing the material demand for laser power and enhancing the material absorption rate of the laser. This increases the depth of fusion, enhances the welding speed, and improves the quality of the welding. However, due to the instability of the welding process, excessive spatter, humping, and porosity can occur, which seriously limit further development of this technology. The existence of pores inside the weld necessitates the use of instruments for detection, which increases the difficulty of detection and weakens the effective working section of the weld; this negatively impacts the strength and toughness of the joint. Studying the influence of porosity in composite welding is important for further understanding the physical process of laser-arc composite welding and the optimization of composite welding process parameters. In this study, the influence of laser-to-steam on composite welding keyhole porosity was investigated by linearly varying the laser power during the welding process. Subsequently, in combination with high-speed camera observation of the composite welding plasma morphology, the impact of the arc on the keyhole porosity was studied. Finally, considering the weld depth, weld width, weld formation and variation rules of porosity in the weld, the formation rules and influencing factors of keyhole porosity in the weld during the fiber laser-TIG hybrid welding were analyzed to establish the theoretical foundation for optimizing the laser-arc hybrid welding technology and understanding the energy coupling mechanism in laser-arc hybrid welding process.

Methods The distribution of internal pores in the weld was first observed at different arc currents using a linearly varying laser power composite welding method. Then, the distribution of internal pores in the weld using fixed laser power composite welding and linearly varying laser power composite welding was compared, proving that the linearly varying laser power approach is feasible. Subsequently, the plasma morphology, surface morphology and internal porosity distribution of the weld were analyzed using a high-

speed camera and an ultra-deep field microscope under different arc currents. Finally, the weld formation, weld depth, and weld width at different currents were compared by linearly varying the laser power.

Results and discussions Almost no pores are observed in the weld during fiber laser welding; there is only the effect of laser-induced steam on the molten pool of the keyhole wall in the deep penetrating keyhole. It is more conducive to improving the stability or maintenance of the keyhole than the existence of an arc. The keyhole does not collapse; therefore, the more laser-induced steam in the hole, the fewer pores in the weld (Fig. 2). A comparative experiment was conducted, and the results showed that the distribution trend of the pores in the weld was the same when the linearly varying laser power composite welding and the fixed laser power were used (Fig. 3). The greater the force of the arc on the molten pool (i. e. , the greater the shielding gas flow rate), the more likely the deep penetration holes will be unstable and collapsed, and the more pores are in the weld (Figs. 6, 7). In the fiber laser-TIG hybrid welding, the penetration width and penetration depth are significantly improved compared with single fiber laser welding, and the surface forming quality of the weld and the spatter effect are significantly improved, as shown in Figs. 8, 9. When the laser power is between 0.8 and 2 kW, the laser power is roughly equivalent to the arc power, that is, the hybrid welding mode at this stage changes from the laser-assisted type to the laser-based type. At this time, the force of the arc acting on the convex liquid column on the rear wall of the small orifice cannot be ignored compared with the eruption of the steam caused by the laser in the hole. The force will press the convex liquid column behind the small orifice to the small orifice when the arc acts on the small hole and the force along the convex liquid column is too large (Fig. 11).

Conclusions In the composite welding process, we obtained the variation law of small pores in the weld with the laser power, when the laser power increases linearly from 0 to 3 kW within 2 s. No pores were observed inside the weld when the laser power was less than 0.8 kW and more than 2.2 kW. When the laser power was approximately 0.8–2.2 kW or the shielding gas flow rate was more than 15 L/min, more pores were seen inside the weld. These pores were distributed in the middle of the weld. The introduction of the TIG arc significantly improved the surface formation of the weld seam in fiber laser welding and substantially increased the melt depth and melt width. When the laser power was 2 kW, the TIG arc at 150 A increased the depth width by 94% and the melt depth by 35%. In fiber laser-TIG arc hybrid welding, the formation of small hole-type pores in the weld is caused by the arc acting on the small orifice, which results in instability and collapse of the small hole. Increasing the shielding gas flow can significantly increase the porosity in the weld. The change in laser-induced evaporation in the hole caused by the change in laser power is the main factor that causes the change in the number of pores in the hybrid welding seam.

Key words laser technique; fiber laser; hybrid welding; small hole-type porosity; process parameters